

URTeC: 3694645

Experimental Evaluation of Enhanced Tight Oil Recovery Performance by Microbubble CO₂ and Microbubble Rich Gas in North Dakota Plays

Yang Yu^{*1}, Christopher Beddoe¹, Ziqiu Xue², Alexander Chakhmakhchev¹, John Hamling¹, Steven Smith¹, Bethany Kurz¹, 1. Energy and Environmental Research Center, 2. The Research Institute of Innovative Technology for the Earth.

Copyright 2022, Unconventional Resources Technology Conference (URTeC) DOI 10.15530/urtec-2022-3694645

This paper was prepared for presentation at the Unconventional Resources Technology Conference held in Houston, Texas, USA, 20-22 June 2022.

The URTeC Technical Program Committee accepted this presentation on the basis of information contained in an abstract submitted by the author(s). The contents of this paper have not been reviewed by URTeC and URTeC does not warrant the accuracy, reliability, or timeliness of any information herein. All information is the responsibility of and is subject to corrections by the author(s). Any person or entity that relies on any information obtained from this paper does so at their own risk. The information herein does not necessarily reflect any position of URTeC. Any reproduction, distribution, or storage of any part of this paper by anyone other than the author without the written consent of URTeC is prohibited.

Abstract

Tight oil plays have emerged as dominant producers, contributing 65% of domestic crude oil production in 2021, with the Bakken play being one of the top three oil-producing plays in the United States. Previous lab work has demonstrated that rich gas and CO₂ will permeate into Middle Bakken core samples under reservoir conditions and mobilize upward of 90% of the hydrocarbon present. For conventional oil plays, microbubble CO₂ injection has been shown to reduce viscous fingering and improve sweep efficiency in both lab and field injection tests. This research applies the technique in rock samples from unconventional oil plays. This study aims to evaluate and compare the recovery performance of microbubble gas injection and continuous gas injection in tight formations in North Dakota.

Core flooding tests were conducted on rock plugs saturated with dead Bakken oil to evaluate the recovery process and compare recovery factors (RF). Core samples were collected from the Red River and Bakken Formations, with permeabilities of 9 mD and 246 nD, respectively. Two gases were used for flooding: CO₂ and a rich gas mixture. Both nonmicrobubble and microbubble gas flooding was performed on the Red River plug. For the Bakken plug, continuous gas flooding was tested. Additionally, a study was performed to evaluate the recovery performance between two types of CO₂ flooding processes (conventional and microbubble) on the Red River plug by using X-ray computed tomography to visualize the displacement history during the tests.

For the Red River plug, results showed that CO₂ injection greatly outperformed rich gas regardless of flooding process. Both RF and visualization results suggest that microbubble CO₂ has better recovery performance than continuous CO₂. A higher differential pressure (ΔP) was generated during the microbubble CO₂ process, which contributed to the additional recovery. While testing with rich gas, both processes produced similar amounts of oil. The ΔP profiles from both processes were very similar, with no major variation. For the Middle Bakken plug, conventional CO₂ flooding produced 14% more oil than the rich gas injection. Because of the ultralow matrix permeability and limited pore volume, further testing of the microbubble process in fractured Bakken plugs is recommended.

This study effort was undertaken to 1) provide a first-of-a-kind evaluation of a microbubble CO₂ enhanced oil recovery (EOR) technique for application in tight unconventional plays, 2) compare the performance of microbubble CO₂ injection with continuous-phase CO₂ injection for Red River EOR applications in North Dakota, and 3) investigate the effectiveness and feasibility of microbubble EOR by using a rich gas mixture in low-permeability formations to assess microbubble rich gas EOR performance relative to microbubble CO₂ EOR performance.

Introduction

According to the U.S. Energy Information Administration (2022), about 65% of domestic crude oil was produced directly from tight oil resources in 2021. Unconventional oil plays have emerged as dominant producers, with the Bakken play being one of the top three oil-producing plays in the United States. The North Dakota Department of Mineral Resources (Helms, 2019) estimated between 25,000 and 70,000 additional wells will be required to fully develop primary production of the Bakken. Even so, production trends and decline curve analysis suggest primary recovery will only produce ~10% of the 300 to 900 billion barrels of original oil in place (OOIP). The Red River Formation is another prolific producer of oil and gas in North Dakota, with production exceeding 300 million barrels from 1300 wells. The Red River's cumulative oil production is the third highest for the state and is only surpassed by the Bakken–Three Forks Formations (>1.2 billion barrels of oil) and the Madison Group (>1 billion barrels of oil) (Nesheim, 2017a). Nesheim (2017b) estimated that various zones in the Red River Formation have collectively generated over 50 billion barrels of oil beneath western North Dakota. Application of water flooding, a common secondary recovery technique, is generally accepted as not being viable for enhancing production from unconventional reservoirs because of low permeability and porosity of the formations. Rich gas and CO₂ enhanced oil recovery (EOR) show promise as a Bakken incremental oil recovery (IOR) technique (National Energy Technology Laboratory, 2010). Development and application of more effective IOR techniques will create tremendous potential to prolong the operational lifetime of existing wells and increase the ultimate recovery from tight formations.

Previous laboratory work has demonstrated that rich gas and CO₂ exposure to Bakken core samples under reservoir conditions may mobilize upward of 90% of the hydrocarbon present (Hawthorne et al., 2017; Jin et al., 2017; Sorensen et al., 2017). Similarly, physics-based reservoir simulations of Bakken multiwell cyclic huff 'n' puff scenarios suggested that rich gas and CO₂-based EOR can more than double the estimated ultimate recovery (EUR) of a drill spacing unit, albeit production response is delayed compared to EOR in conventional reservoirs. These findings have been corroborated through a field-based CO₂ injection test that was conducted in collaboration with XTO Energy in 2017. During the test, ~100 tons of CO₂ was injected over 5 days into an unstimulated Middle Bakken reservoir. While the permeation rate into the matrix was presumed to be low, the chemical composition of produced oil before and after the test demonstrated that the injected CO₂ mobilized oil from the Middle Bakken matrix that would otherwise not be mobile under primary production. At the time of publishing, limited data sets are available for CO₂ EOR core flooding studies conducted on Red River samples.

Challenges facing unconventional EOR implementation that weaken recovery performance include gravity override of the injected CO₂ (density difference between injected CO₂ and residual fluids), viscous fingering that results in reduced sweep efficiency, the presence of high-permeability fracture networks which results in bypass of the reservoir matrix and high utilization rates from loss of EOR fluid (Meyer, 2007), and low permeation rates that suppress or delay response. The Research Institute of Innovative Technology for the Earth (RITE) has developed a technology for injecting CO₂ as microbubbles (bubble diameter less than 1 millimeter) (Xue et al., 2014, 2018; Yamabe et al., 2013) to improve EOR performance. Microbubble CO₂ injection has been shown to reduce viscous fingering and improve sweep efficiency in both laboratory and field injection tests. The buoyancy of microbubble CO₂ relative to brine is significantly reduced compared to continuous supercritical-phase CO₂, suggesting that the tendency for gravity override near an injection well may be slowed or delayed. Furthermore, field injection data show

that achievable injection rates into a ~50-mD sandstone can be doubled through use of microbubble CO₂ injection compared to continuous supercritical CO₂ injection. These technical benefits are applicable to both EOR (i.e., improved sweep, increased EUR) and geologic CO₂ storage potential (i.e., increased injectivity, improved storage efficiency), both of which provide direct benefit to EOR and CCS (carbon capture and storage) projects across the nation.

Core flooding tests were conducted to evaluate recovery processes and compare the recovery factor (RF) using CO₂ and a rich gas mixture to flood core plugs collected from the Middle Bakken and Red River Formations in North Dakota. Both of the formations represent tight plays with low permeability. The production achieved during experimentation was determined through direct observation of the collected oil or the mass loss of the tested plug. Additionally, the recovery performance of two CO₂ flooding processes in the Red River sample was evaluated by using an X-ray computed tomography (CT) scanner, which allowed for visualization of the fluid distribution and displacement history during the tests.

This study aimed to 1) evaluate a microbubble CO₂ EOR technique for application in tight unconventional plays, with matrix permeabilities in the low microdarcy and nanodarcy range; 2) compare the performance of microbubble CO₂ injection with continuous-phase CO₂ injection in samples from the Red River Formation; and 3) investigate the effectiveness and feasibility of microbubble EOR by using a rich gas mixture in low-permeability formations to assess microbubble rich gas EOR performance relative to microbubble CO₂ EOR performance.

Experimental Work

Samples

Core plugs were drilled from the Red River and Middle Bakken Formations which represent plays with low microdarcy and nanodarcy permeability, respectively. Multiple samples were collected from each interval and then scanned by X-ray micro-CT to evaluate internal structure and examine mechanical integrity and consistency of the samples. The selected samples for core flooding tests were relatively homogeneous and had no visual internal fractures. Porosity for selected plugs was measured using a gas porosimeter and applying Boyle's law. The permeability of the Red River plug was determined by a steady-state method using Darcy's law, whereas the permeability for the tight Bakken plug was measured using the pulse-decay method.

To achieve the most comparable results, the Red River sample was cut in half as identified by the -1 and -2 in the sample numbers. One half (No. 129690-1) was used to evaluate the recovery performance of CO₂ flooding using an X-ray CT scanner. The second half of the Red River plug (No. 129690-2) and the Bakken plug (No. 116231) were used to implement flooding tests using the two gases and to evaluate the recovery efficiency quantitatively by recovery factor. Table 1 shows the measured properties of the samples selected for testing.

Table 1. Properties of Core Plug Samples

Sample No.	Formation	Length (cm)	Diameter (cm)	Mass (g)	Pore Vol. (cm ³)	Porosity (%)	Permeability (mD)
129690-1	Red River	4.280	3.015	69.521	6.101	19.97	3.98
129690-2	Red River	4.630	3.015	74.740	26.203	20.73	9.07
116231	Middle Bakken	3.507	3.015	65.421	0.616	2.46	0.000246

The oil sample used for core plug saturation was dead Bakken oil with a density of 0.815 g/cm³ under 72°F (22°C) and atmospheric pressure. Two types of gas were used in the core flooding tests: a CO₂ and a rich gas mixture consisting of 70% methane, 20% ethane, and 10% propane.

Experimental Design

The experimental work consisted of two parts: a) core plug saturation and b) the gas flooding process.

Core Saturation. Prior to the core flooding test, dried core samples were vacuumed and then saturated with dead oil. For the Red River plug, the sample was saturated with oil using a desiccator. For the Bakken plug, the saturation process was performed under high pressure to achieve the maximum performance. Figure 1 shows the schematic of the setup used for tight core sample saturation as referred to in Yu et al. (2016). The core sample was placed in a stainless steel, high-pressure vessel. A vacuum pump was used to evacuate air remaining in the vessel and the pore spaces of the core plug. The vacuum was maintained for 1 day to sufficiently evacuate the tight pore space. A syringe pump (Teledyne ISCO) connected with an accumulator was used to transfer the oil to the vessel under a constant pressure of 3000 psi for at least 24 hours at 104°F (40°C). These conditions were identical to those of the core flooding process. After saturation, the system pressure was released, and the sample was kept in the vessel for several hours to equalize the sample pressure. The plug was then removed from the vessel, the excess oil residue was wiped from the outside of the sample, and the mass of the oil-saturated plug was measured.

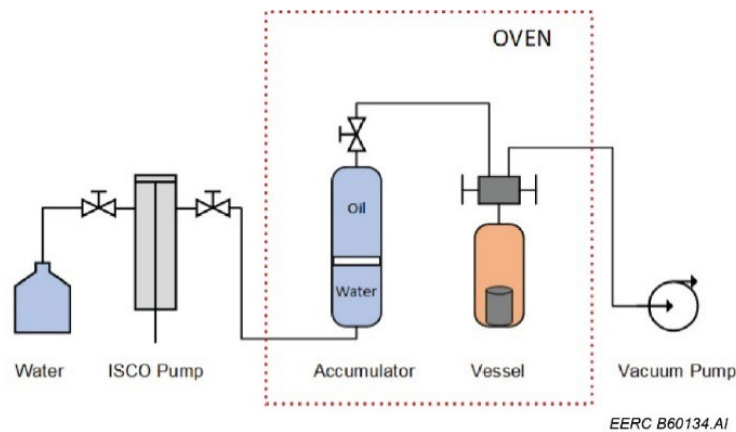


Figure 1. Schematic of system used for saturation of tight core plugs.

The degree of oil saturation of the plug was evaluated after each saturation process to ensure that the core reached a maximum and consistent saturation. Oil saturation equals the ratio of the volume of saturated oil (oil-in-place) to the pore volume (PV) of the plug. The oil-in-place was calculated from the mass difference between the dry and saturated core divided by the density of the oil sample. The reference PV is determined by Boyle's law using a gas porosimeter. Using these procedures, a consistent level of core saturation was maintained throughout all tests on a given sample.

Core Flooding. Once the core plug saturation was completed, two types of flooding processes were performed on the same core plug under the same test conditions: a conventional gas flood and a microbubble gas flood. For the conventional flood, the core sample was placed in the core holder inside a rubber sleeve, to accommodate confining pressure and back pressure, before gas was injected into the plug. For the microbubble flooding process, a porous disc was used to generate microbubbles at the inlet of the core, as shown in Figure 2. This microbubble frit was initially fully saturated with water, and the microbubbles were generated as gas was injected through it. A diagram of the system used is shown in Figure 3.

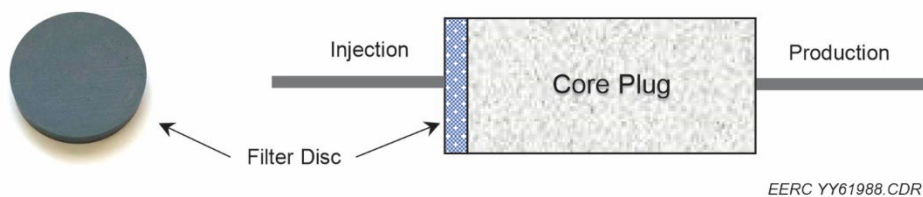


Figure 2. Special designed filter placed at the inlet for microbubble gas injection.

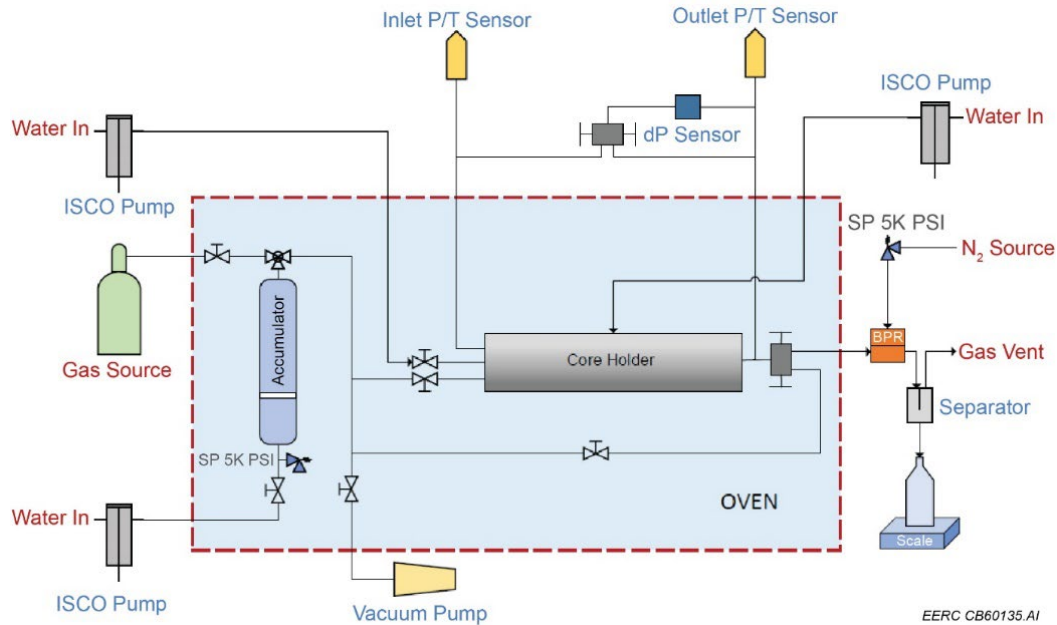


Figure 3. Schematic of the gas flooding system.

Based on the sample properties, different injection modes were used for the flooding process, and different methods were used to measure the recovery factor. For the conventional plug, a constant injection rate was applied. For the tight sample with ultralow permeability, the flooding process could only be conducted by injecting fluid under constant pressure conditions because of the poor injectivity, and a desired lower backpressure was set to create the differential pressure. All tests were performed at a temperature of 40°C. When no additional oil was produced, flooding tests were terminated. Table 2 presents the specific test conditions for each sample.

Table 2. Test Conditions for Each Sample and RF Determination Method

Sample Type and ID	Operating Condition	RF Determination Method
Red River 129690-2	<ul style="list-style-type: none"> Constant injection rate 1 cm³/min Confining pressure 3500 psi Backpressure 3000 psi Conventional and microbubble gas flooding 	Measure the mass of produced liquid using an analytical balance to determine the recovery history and ultimate RF.
Middle Bakken 11623	<ul style="list-style-type: none"> Constant inlet pressure 3000 psi Confining pressure 3500 psi Backpressure 2000 psi Conventional gas flooding only 	Because of the low pore volume, the produced fluid was unable to be collected and quantified in a reliable manner. Instead, RF was determined based on the mass difference of the sample measured before and after the flooding test.

Visualization of the Flooding Process

As a joint comparative study performed by RITE, the recovery performance of CO₂ flooding on Red River Plug No. 129690-1 was examined by using an X-ray CT scanner. In this work, the sample was placed in a core holder and saturated with artificial brine at a confining pressure of 18 MPa (2610 psi) and

a pore pressure of 10 MPa (1450 psi). The sample was then flooded with decane until no brine was discharged to simulate the oil reservoir condition. The microbubble CO_2 process was performed initially, after which the sample was cleaned and reused for the nonmicrobubble continuous CO_2 flooding. The CO_2 was injected into the plug with a constant flow rate of $0.1 \text{ cm}^3/\text{min}$. Both flooding processes were scanned to visualize the fluid distribution and displacement history.

Results and Discussion

Red River Sample No. 129690-2

CO₂ Flooding. Figure 4 shows the RF profile calculated using the mass of produced oil. It shows a 7% improvement in ultimate recovery using microbubble vs. nonmicrobubble CO_2 injection into the Red River core. The microbubble CO_2 , with a faster production rate, yielded more oil than nonmicrobubble throughout the flooding process. Figure 5 shows the differential pressure (ΔP) profile for the nonmicrobubble and microbubble CO_2 tests. The microbubble process was able to generate a higher ΔP , which contributed to the increased oil recovery. Based on the evaluation of ΔP , the authors believe that the microbubble technology restricts the flow of CO_2 through the pore space, which acts to reduce fingering and preferential flow. The increased fluctuation in the ΔP suggests there is increased resistance of the microbubbles moving through the pore space. As these bubbles restrict flow through pore throats, pressure spikes are generated.

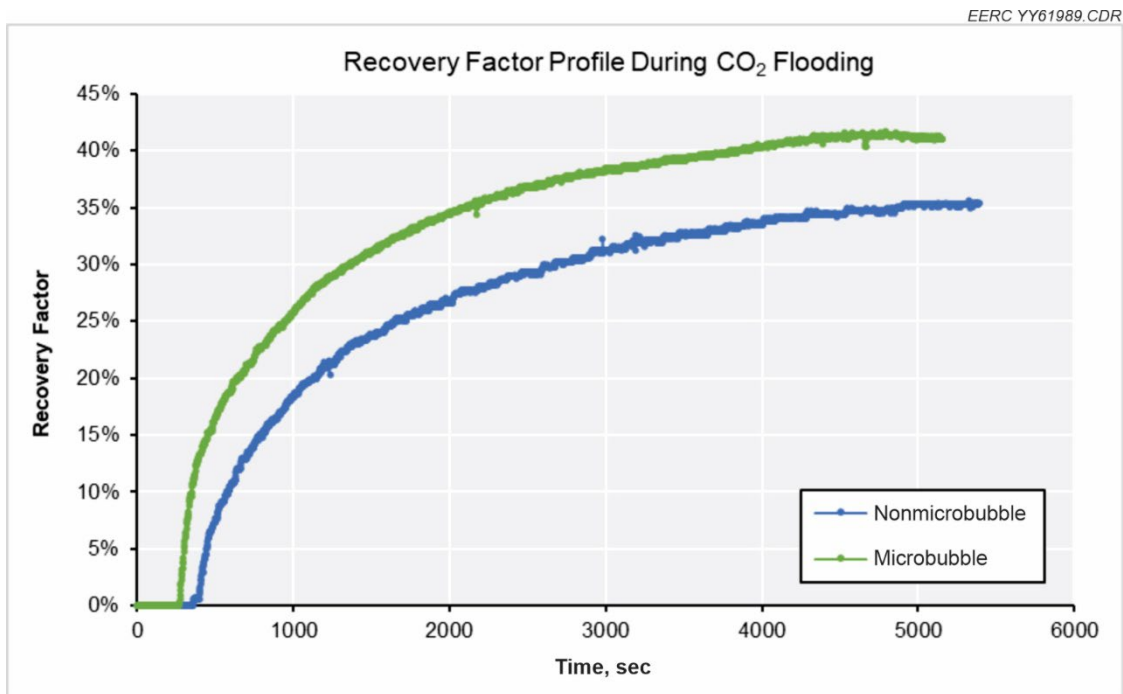


Figure 1. Recovery history profile during CO_2 flooding of Red River Sample No. 129690-2.

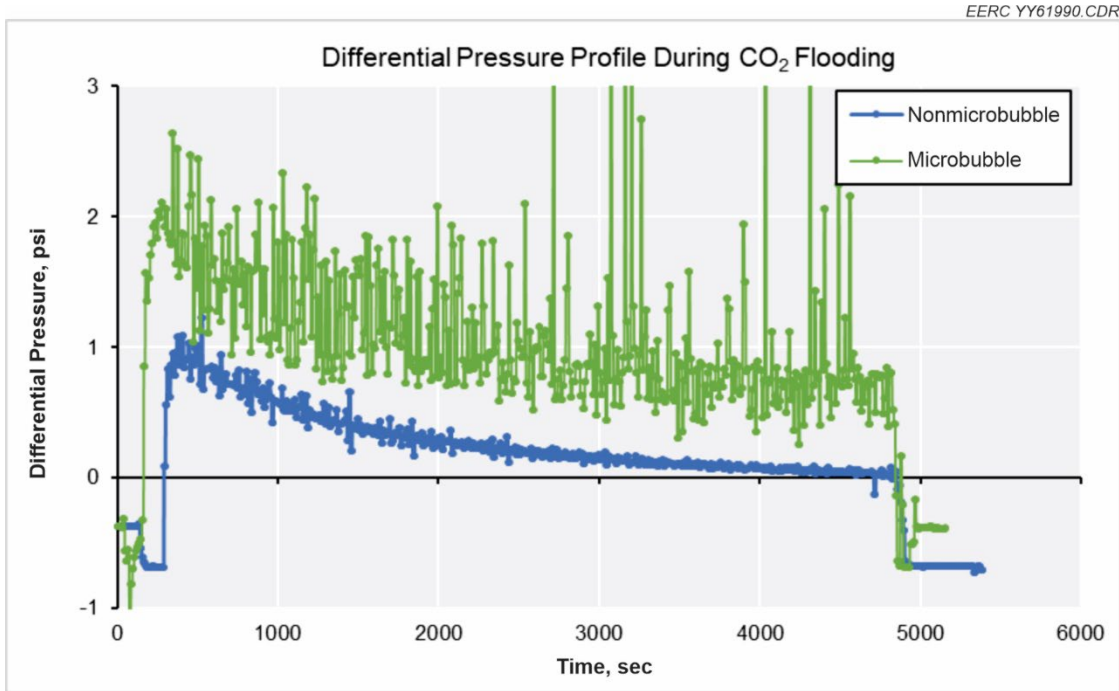


Figure 5. Differential pressure profile during CO₂ flooding of Red River Sample No. 129690-2.

Rich Gas Flooding. Figure 6 depicts the recovery history profile of the two flooding processes in the Red River plugs using rich gas. The ultimate RF is reduced by almost 20% when rich gas microbubble injection (22%) is used compared to that of the CO₂ microbubble injection (42%). There was no significant increase in ΔP when using microbubble vs. nonmicrobubble injection with rich gas, as shown in Figure 7. This directly supports the observation in Figure 6, showing essentially no performance gain from microbubble injection of rich gas into the Red River plug.

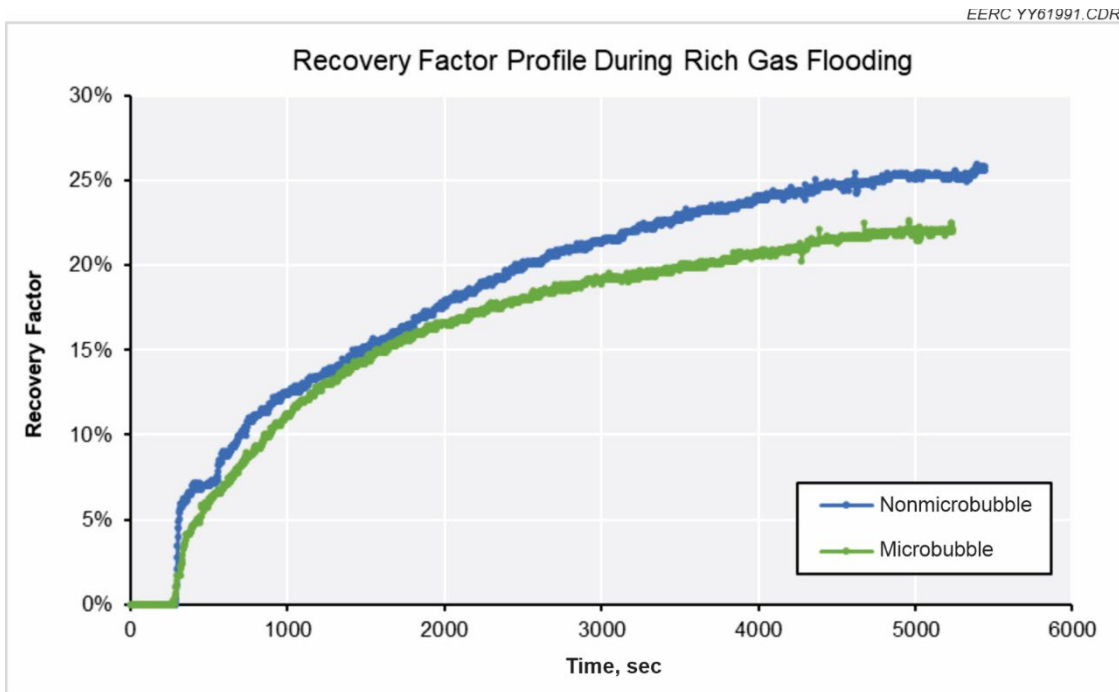


Figure 6. Recovery history during rich gas flooding of Red River Sample No. 129690-2.

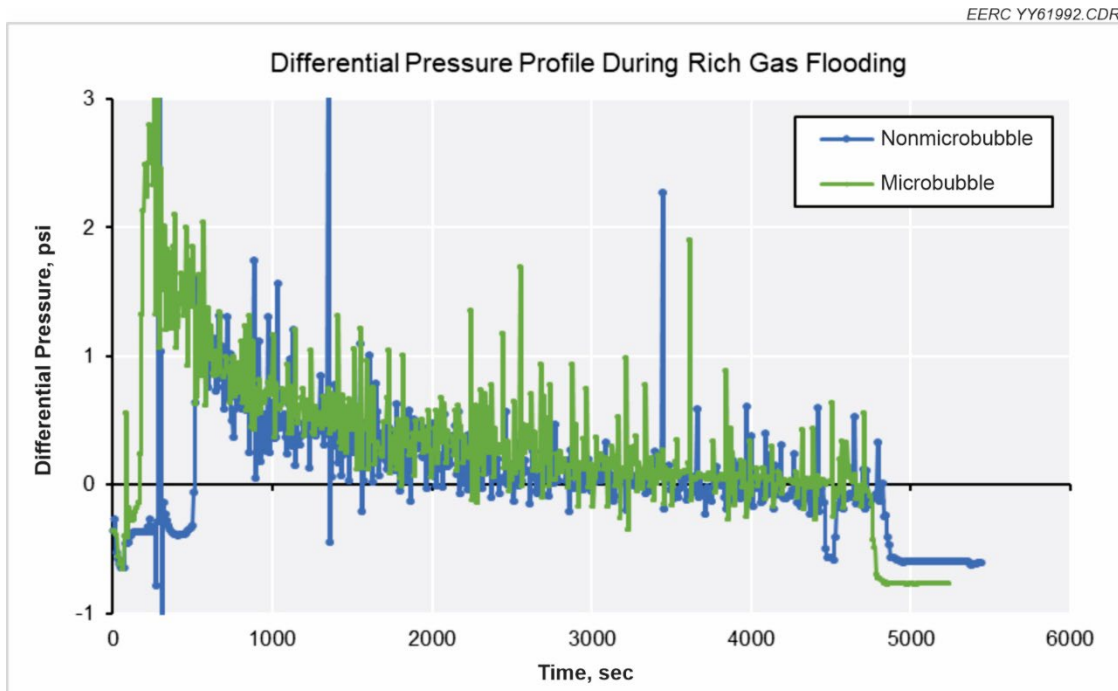


Figure 7. Differential pressure profile during rich gas flooding of Red River Sample No. 129690-2.

Within the tests described herein, CO₂ significantly outperformed rich gas in both the continuous nonmicrobubble CO₂ flood and the microbubble CO₂ flood. Specifically, the CO₂ produce approximately 10% and 20% better recovery than rich gas under nonmicrobubble and microbubble injection, respectively.

CO₂ vs. Rich Gas Microbubble Flooding. The same filter disc was used to generate microbubbles for the CO₂ and rich gas core flood experiments. The reduced RF that was observed for the microbubble rich gas displacement when compared to the microbubble CO₂ displacement may be (at least in part) a result of the pore size of the filter disc being more optimized to generate microbubbles using CO₂ and less optimized to generate microbubbles using rich gas because of differences in the fluid properties. Additional work is required to determine if optimizing of the filter disc properties would have a meaningful influence on the relative RF performance between the microbubble CO₂ vs. microbubble rich gas scenarios.

Red River Sample No. 129690-1

For this sample, the recovery efficiency of the nonmicrobubble CO₂ and microbubble CO₂ injection was examined by X-ray CT to scan and visualize CO₂ migration within the plug throughout the test. The same plug was used for both recovery processes. Prior to each flooding test, the sample was saturated with artificial brine while in the core holder and then injected with decane until no incremental brine was displaced and irreducible water was achieved to simulate a reservoir condition. The processed CT images of the sample, with the legend showing change in CT numbers (ΔCT), from both processes are presented in Figure 8. The changes in color (from dark blue to dark red) represent the changes of average density in the corresponding area. As the color begins changing from dark blue to a lighter color (increase in ΔCT), this indicates that the CO₂ has started migrating into the plug and begun displacing the in-place fluids (brine and decane). As the color changes from lighter blue to yellow, orange, and red colors (or greater ΔCT), it indicates that more of the in-place fluids have been discharged by the CO₂. The analysis of the flooding tests using X-ray CT allowed the research team to understand the CO₂ distribution and displacement history and efficiency during the test.

Figure 8. Comparative CT Images of nonmicrobubble CO₂ and microbubble CO₂ flooding on Red River Sample No. 129690-1 resulting from the core flooding work performed by RITE (continued).

EERC YY61994.CDR

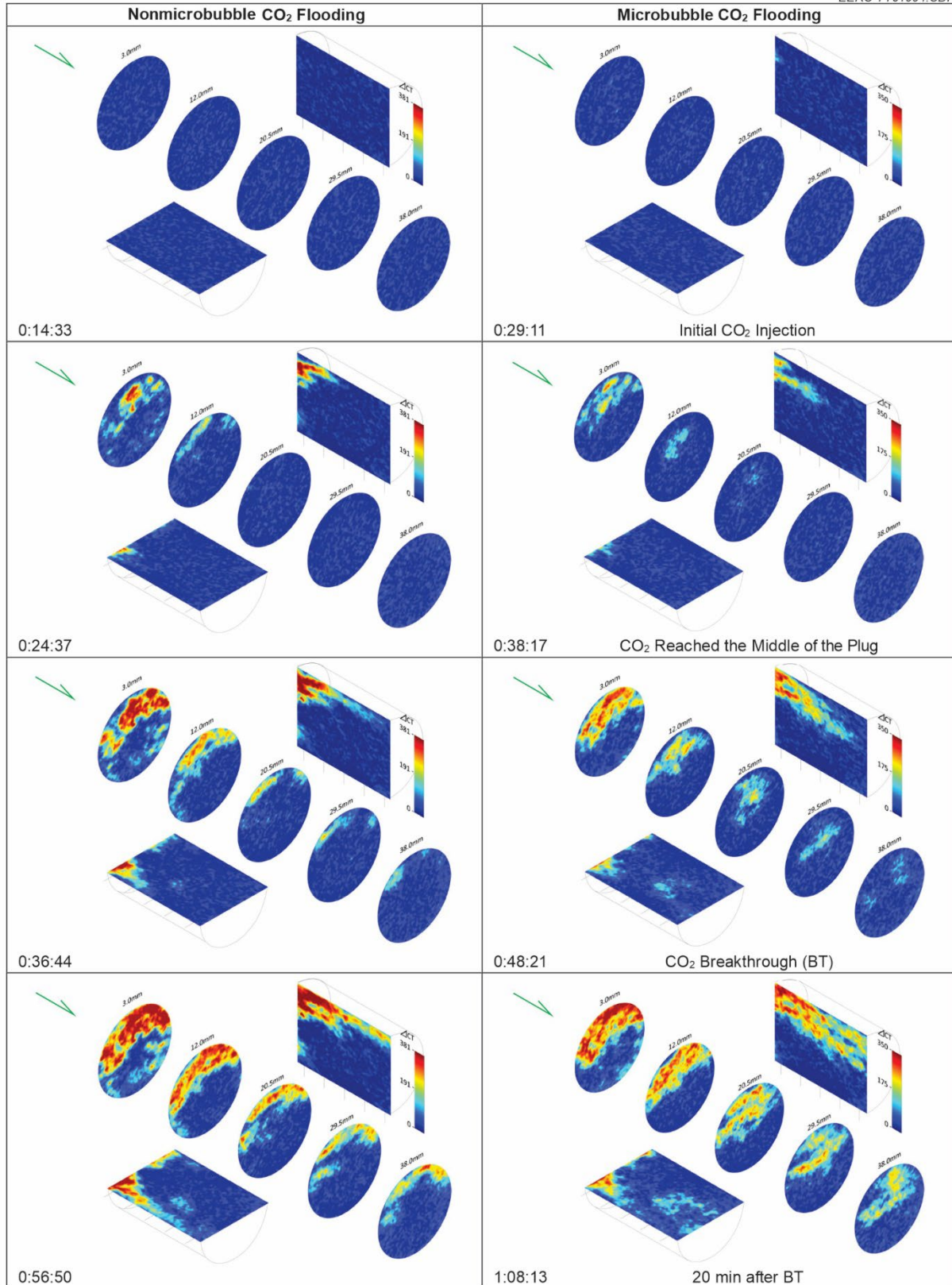
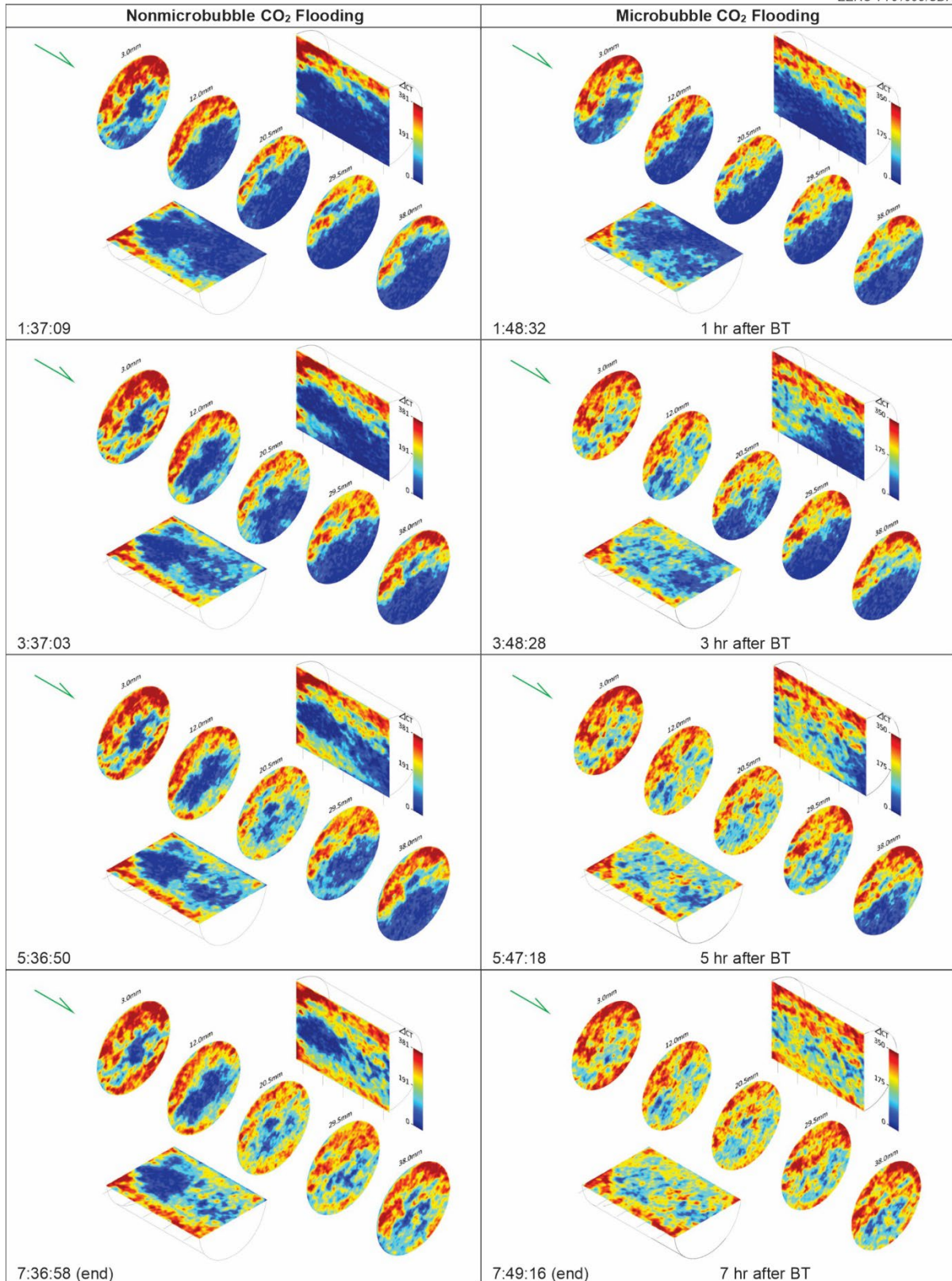


Figure 8 cont. Comparative CT Images of nonmicrobubble CO₂ and microbubble CO₂ flooding on Red River Sample No. 129690-1 resulting from the core flooding work performed by RITE

EERC YY61995.CDR



As shown in the horizontal cross-section images that parallel the flow direction of the injection fluid, especially after breakthrough (BT), the microbubble CO₂ flooding outperforms the nonmicrobubble CO₂ process on displacing the saturated fluids. The blue area in the microbubble CO₂ was dramatically reduced at the end of the test compared to nonmicrobubble CO₂ flooding.

Middle Bakken Sample

Figure 9 shows and compares the ultimate RF results of continuous gas injection in the Middle Bakken sample by CO₂ and rich gas, respectively. As mentioned earlier, the RF is calculated from Eq. 1:

$$RF = \frac{W_{sat} - W_{exp}}{W_{sat} - W_{dry}} \quad (1)$$

where W_{sat} is the mass of oil-saturated sample measured before the test; W_{exp} is the mass of the sample measured after the flooding test; W_{dry} is the mass of dry core sample.

The results show that the CO₂ process recovered 52.3% of the OOIP, approximately 14% more production than the rich gas flooding. Because of the poor injectivity in the Bakken plug and the challenge of obtaining real-time oil recovery, the microbubble CO₂ process was not able to be evaluated using the matrix plug in this study. For future work, we recommend performing the comparative examination on the recovery efficiency of microbubble CO₂ and nonmicrobubble CO₂ processes in fractured ultratight samples. Such a scenario can better simulate actual reservoir conditions and may offer improved fluid injectivity as well as greater pore volume, which could also potentially reduce experimental errors and uncertainties.

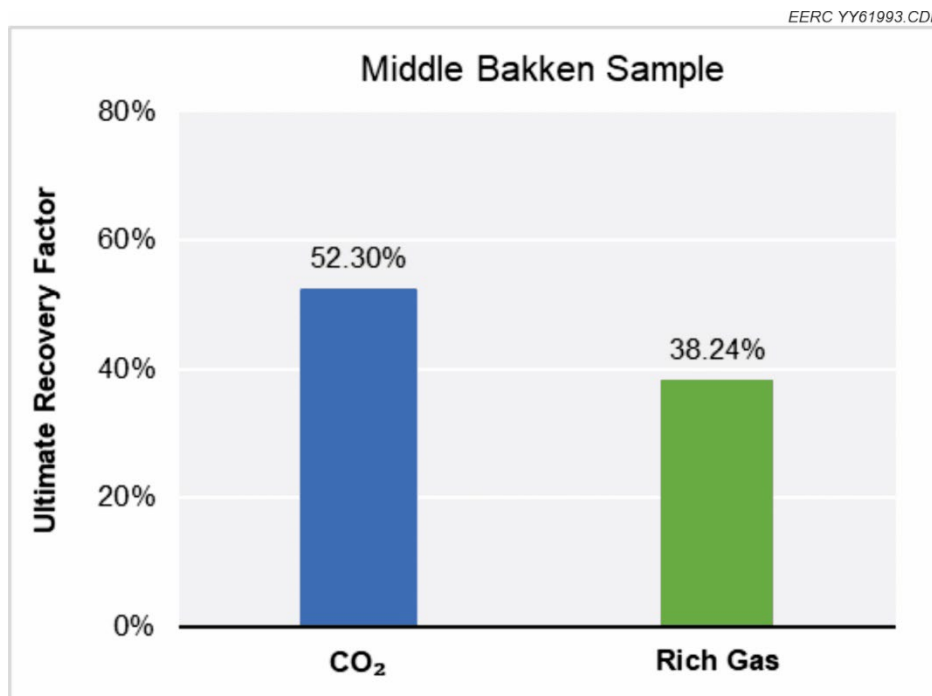


Figure 9. Ultimate recovery factor results for Middle Bakken Sample No. 116231 ($k = 246$ nD).

Conclusions

In this study, core flooding tests were conducted to evaluate the EOR effectiveness of microbubble gas injection technology in tight formations for comparison with nonmicrobubble gas injection:

- Within the Red River Formation samples, the microbubble CO₂ process outperformed the nonmicrobubble continuous CO₂ injection. Based on the recovery history and visualization of CT images during the flooding period, a higher ΔP can be achieved, and the displacement efficiency can be significantly improved during the microbubble CO₂ process compared to conventional CO₂ injection.
- The performance of the microbubble rich gas flooding in the Red River plug was not as effective as the microbubble CO₂ process on improving oil recovery as opposed to the nonmicrobubble process. Both processes show similar variation profiles in ΔP during the recovery history.
- The recovery performance by using different gases may be associated with the properties of the filter disc. Further work is required to determine if optimizing of the filter disc properties would have a meaningful influence on the relative RF performance between the microbubble CO₂ vs. microbubble rich gas scenarios.
- The continuous CO₂ flooding of the Middle Bakken sample yielded 14% more oil than the rich gas flooding.
- A comparative study testing the recovery performance of microbubble CO₂ and nonmicrobubble CO₂ processes in other tight reservoirs, such as the Bakken Formation, is recommended for better simulating the reservoir conditions. In addition, tests should be performed using both, fractured and unfractured, samples to evaluate the difference in microbubble gas performance.

Acknowledgments

This research was funded by the State Energy Research Center of North Dakota.

References

- Hawthorne, S.B., Jin, L., Kurz, B.A., et al. 2017. Integrating Petrographic and Petrophysical Analyses with CO₂ Permeation and Oil Extraction and Recovery in the Bakken Tight Oil Formation. Paper presented at the SPE Unconventional Resources Conference, Calgary, Alberta, Canada, 15-16 February. SPE-185081-MS. <https://doi.org/10.2118/185081-MS>.
- Helms, L.D. 2019. House Energy and Natural Resources Committee: Presentation to 66th Legislative Assembly, Department of Mineral Resources, North Dakota Industrial Committee. 10 January. https://www.dmr.nd.gov/oilgas/presentations/HouseEnergyNaturalResources011019_25.pdf.
<https://www.dmr.nd.gov/ndgs/documents/newsletter/2017Winter/Oil%20and%20Gas%20Potential%20of%20the%20Red%20River%20Formation,%20Southwestern%20North%20Dakota.pdf>
https://www.dmr.nd.gov/ndgs/documents/Publication_List/pdf/GEOINV/GI-196.pdf.
- Jin, L., Sorensen, J.A., Hawthorne, S.B. et al. 2017. Improving Oil Recovery by Use of Carbon Dioxide in the Bakken Unconventional System: A Laboratory Investigation. *SPE Res Eval & Eng* **20** (03): 602–612. SPE-178948-PA. <https://doi.org/10.2118/178948-PA>.
- Meyer, J.P. 2007. Summary of Carbon Dioxide Enhanced Oil Recovery (CO₂ EOR) Injection Well Technology. American Petroleum Institute, Washington, DC.

- National Energy Technology Laboratory. 2010. Carbon Dioxide Enhanced Oil Recovery—Untapped Domestic Energy Supply and Long-Term Carbon Storage Solution. March 2010. www.netl.doe.gov/sites/default/files/netl-file/co2_eor_primer.pdf.
- Nesheim, T.O. 2017a. Oil and Gas Potential of the Red River Formation, Southwestern North Dakota. North Dakota Geological Survey.
- Nesheim, T.O. 2017b. Stratigraphic and Geochemical Investigation of Kukersites (petroleum source beds) Within the Ordovician Red River Formation, Williston Basin. *AAPG Bulletin* **101** (9): 1445–1471. <https://doi.org/10.1306/11111616075>.
- Sorensen, J.A., Kurz, B.A., Hawthorne, S.B. et al. 2017. Laboratory Characterization and Modeling to Examine CO₂ Storage and Enhanced Oil Recovery in an Unconventional Tight Oil Formation. *Energy Procedia* 114: 5460–5478. <https://doi.org/10.1016/j.egypro.2017.03.1690>.
- U.S. Energy Information Administration (EIA). 2022. How Much Shale (Tight) Oil Is Produced in the United States? <https://www.eia.gov/tools/faqs/faq.php?id=847&t=6>.
- Xue, Z., Nishio, S., Hagiwara, N. et al. 2014. Microbubble Carbon Dioxide Injection for Enhanced Dissolution in Geological Sequestration and Improved Oil Recovery. *Energy Procedia* **63**: 7939–7946. <https://doi.org/10.1016/j.egypro.2014.11.828>.
- Xue, Z., Park, H., Ueda, R. et al. 2018. Microbubble CO₂ Injection for Enhanced Oil Recovery and Geological Sequestration in Heterogeneous and Low Permeability Reservoirs. Paper presented at the 14th Greenhouse Gas Control Technologies Conference, Melbourne, Australia, 21–26 October.
- Yamabe, H., Nakaoka, K., Xue, Z. et al. 2013. Simulation Study of CO₂ Micro-Bubble Generation Through Porous Media. *Energy Procedia* **37**: 4635–4646. <https://doi.org/10.1016/j.egypro.2013.06.372>.
- Yu, Y., Meng, X., Sheng, J.J. 2016. Experimental and Numerical Evaluation of the Potential of Improving Oil Recovery from Shale Plugs by Nitrogen Gas Flooding. *Journal of Unconventional Oil and Gas Resources* **15**: 56-65. <https://doi.org/10.1016/j.juogr.2016.05.003>.